Delft University of Technology

Exploring Subsurface Water Conditions in Dutch Canal Dikes During Drought Periods
Insights From Multiyear Monitoring

Strijker, Bart; Heimovaara, Timo J.; Jonkman, Sebastiaan N.; Kok, Matthijs

Water Resources Research®

RESEARCH ARTICLE

Key Points:

- Novel multiyear observations of soil moisture and hydraulic heads from various canal dikes reveal geohydrological behavior
- The precipitation deficit emerges as the most reliable meteorological drought indicator and can be used as an indicator of dike safety
- The drought recovery lasted 4.5 months in 2022, which is important for the transition between seasons and different failure mechanisms

Correspondence to:

B. Strijker,
b.strijker@tudelft.nl

Exploring Subsurface Water Conditions in Dutch Canal Dikes During Drought Periods: Insights From Multiyear Monitoring

Bart Strijker[1,2] , **Timo J. Heimovaara[1]** , **Sebastiaan N. Jonkman[1]** , and **Matthijs Kok[1,2]**

[1]Delft University of Technology, Delft, The Netherlands, [2]HKV Consultants, Lelystad, The Netherlands

Abstract Canal dikes in low-lying polders, as well as in other regions worldwide, are critical infrastructure for flood protection and water management. The subsurface water conditions can cause dike failures during excessive rainfall and prolonged periods of drought. There is a lack of multi-year monitoring of subsurface water conditions in canal dikes and an insufficient understanding of their geohydrological behavior. This study provides and analyses a novel multiyear data set of soil moisture and hydraulic heads (from February 2020 until March 2023) from a monitoring network covering various canal dikes with different characteristics in the western Netherlands. The data, including two extremely dry summers, highlight the impact of meteorological variations on the subsurface water conditions. Non-hydrostatic hydraulic head levels were observed during droughts that can be detrimental to dike stability and that are often not accounted for in safety assessments for drought situations. The effectiveness of various meteorological drought indicators applied to subsurface water conditions was evaluated: the precipitation deficit is the most reliable measure and outperforms the standardized drought indicators (SPEI and SPI). The drought recovery of dikes was analyzed to understand seasonal transitions and the sequence of different failure mechanisms, during dry and wet situations. This analysis also reveals differences between meteorological, soil moisture, and groundwater droughts, highlighting soil's storage capacity after drought and the limitations of meteorological drought indicators as proxies for soil moisture and groundwater. The insights from this study enhance assessments, inspection procedures and the identification of weak spots of dikes and other earthworks of infrastructure.

1. Introduction

Flooding is among the leading climatic threats to people's livelihoods, affecting development prospects worldwide (Jevrejeva et al., 2018). Extensive systems of flood defenses protect flood prone areas worldwide (O'Dell et al., 2021) and the top three countries with the highest relative population exposed to flood risk have to a certain degree flood protection systems (Rentschler et al., 2022). To manage flood risks in an embanked area, the performance of dikes plays a crucial role and several failure mechanisms can induce dike breaching and flooding of the hinterland (Özer, van Damme, & Jonkman, 2019). Key inputs to the assessment of dike performances are the loading conditions and the resistance of dikes. Important factors contributing to the loading conditions are subsurface water conditions, such as hydraulic head levels and soil moisture content, which can trigger failure (Sharp et al., 2013). At the same time, changes in subsurface water conditions also induce weakening processes that reduce the resistance, such as soil-strength reduction, and desiccation cracking (Robinson & Vahedifard, 2016; Stirling et al., 2021; Vahedifard et al., 2016; Vardon, 2015). Therefore, understanding subsurface water conditions in dikes is essential for flood protection in embanked areas.

A special case of an embanked area is a polder, which is a low-lying area enclosed by embankments with an internal drainage system. Polders are present in many parts of the world, like the Netherlands, Bangladesh, Vietnam and China (Martín-Antón et al., 2016; Morton & Olson, 2018; Lendering et al., 2018; Tran & Weger, 2018; Triet et al., 2017; Manh et al., 2013; Warner et al., 2018). Drainage canals in polders drain excess water from the polder to the main water bodies (or vice versa) to mitigate the flood risk and facilitate irrigation. Water levels in the canal, regulated using weirs, sluices and pumping stations, can lie several meters above the surrounding polder area. Dikes along the canals, known as canal dikes, are vital infrastructure in low-lying polders and their performance can either prevent or trigger internal flooding if a breach occurs. The Netherlands has more than 10,000 km of canal dikes (Pleijster et al., 2015), which mainly consist of soft soils (clay and peat) covered with grasses (Lendering, 2018). Important driving forces of the changing subsurface water conditions in these dikes are the meteorological conditions since the outside water levels are almost constant, in contrast to many

other types of dikes where the outside water levels are leading (Rikkert, 2022; Van Baars & Van Kempen, 2009). Both droughts and wet situations can trigger instabilities, as well as the cascading impacts of droughts. In the past, many Dutch canal dike failures occurred due to inner-slope instability (Van Baars & Van Kempen, 2009), like the failures during summers near Wilnis and Terbregge in 2003 and Reeuwijk in 2021. However, this is not limited to the Netherlands and several historic dike failures worldwide highlight the impact of drought conditions on dike integrity, such as failures along the Murray Riverbank in Australia from 2008 to 2010 and at Edenburry in Ireland in 1989 (Bezuijen et al., 2005; Hubble et al., 2014; Pigott et al., 1992; Van Baars, 2005). These events underscore the vulnerability of dikes under extended dry periods worldwide.

Soil-atmosphere interaction can significantly impact the stability of soil structures, making it important for safety assessments (Elia et al., 2017; Vardon, 2015). However, modeling soil-atmosphere processes can be challenging and complex. Several attempts have been made to model the effects of rainfall and evaporation on the phreatic surface in dikes, the level within the dike where the soil is fully saturated with water, using a range of models from simple conceptual ones to coupled agro-meteorological and 2D numerical groundwater flow models (Jamalinia et al., 2019; Rikkert, 2022; Van Esch, 2012). Multi-year measurements of hydraulic head levels in combination with soil moisture in dikes, especially canal dikes, are often lacking, which makes modeling exercises difficult to validate. Therefore, knowledge about the geohydrological behavior and the importance of the soil-atmosphere interaction of canal dikes is currently limited. This makes it challenging to quantify loading conditions and assess flood risk levels properly, not to mention accounting for processes that weaken the dike. Furthermore, Dutch canal dikes that are prone to droughts, whose subsoils consist of peat or organic clay, are inspected during dry summers to detect weak spots and take measures to prevent failures. In practice, water managers have to decide when to start inspections. Various meteorological drought indicators are used as an indicator of dike safety, because measurements within dikes are not widely available. The reliability of meteorological indicators for accurately representing the actual drought conditions in canal dikes (such as soil moisture and hydraulic head levels) is unknown, making it difficult to justify decisions made by water managers. Understanding the geo-hydrological response of various canal dikes leads to more accurate safety and reliability assessments of canal dikes and flood defenses in general. Although the focus of this paper is more on canal dikes throughout the Netherlands, the geohydrological response of these dikes can still be very relevant for similar dikes in low-lying polders and for dikes worldwide. The continuous exposure of canal dikes to high water levels and rainfall, and evaporation makes them valuable sources of potential insights applicable to any dike.

1.1. Objective and Outline

This research provides insights into the geohydrological response of dikes by analyzing multiyear monitoring data with a focus on droughts, based on measurement data from 10 monitoring sites with different characteristics. The applicability of various meteorological indicators, to provide information about the development of drought in dikes, is investigated by comparing these with the observed groundwater and soil moisture levels. Lastly, the recovery from droughts is analyzed, which characterizes the transition between different failure mechanisms, during dry and wet situations.

This paper starts by providing relevant background on drought failure and drought-induced weakening processes and discussing the Dutch situation. Then, the monitoring sites are described, including the dike characteristics and monitoring equipment, after which different concepts of droughts and several drought indicators are introduced. Next, the data analyses of the geohydrological response of dikes are presented. In the discussion, the limitations and relevance of these insights for practical application are discussed, followed by concluding remarks and recommendations.

2. Background and Methodology

2.1. Dike Failure and Drought-Induced Weakening

Catastrophic dike failures occurred throughout history with various causes, like storm surge, ice drift and rainfall or drought, and failure mechanisms, such as overflow and overtopping causing soil erosion, external erosion, piping and inner slope instability (Özer, van Damme, & Jonkman, 2019; Van Baars & Van Kempen, 2009). In general, inner slope instability of predominately earthen dikes occurs when the loading conditions exceed the resistance, which is determined by the soil shear strength. For many dikes along rivers and coasts, inner slope instability occurs due to the infiltration of water into the dike body and its foundation, leading to high pore-water
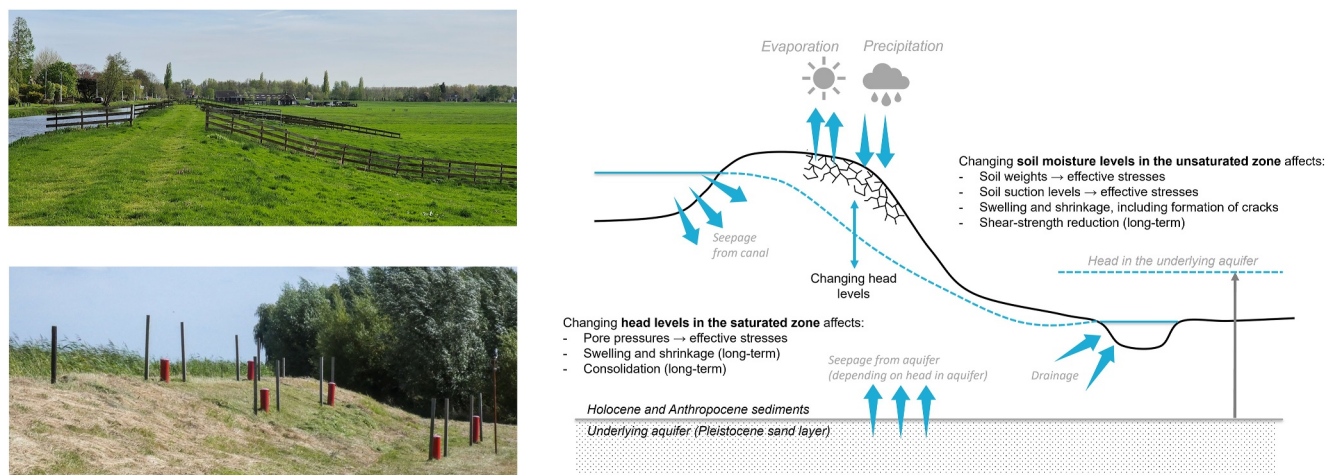
Figure 1. Right side: Conceptual figure that illustrates the subsurface water conditions in canal dikes and the way changing soil moisture and head levels can affect the stability. Left side: Photographs of two canal dikes in the Netherlands, with the MT-polder (top image) and the Duifpolder (bottom image).

pressures, decreasing effective stresses and decreasing the soil shear strength (Frank et al., 2004; Sharp et al., 2013). The infiltration of water into the dike body can be caused by high water levels and heavy rainfall (Rikkert, 2022; Van Baars & Van Kempen, 2009). In addition to failures caused by water infiltration and high pore-water pressures, excessively dry conditions can also induce instabilities. Droughts can affect the stability of dikes in multiple ways, both positive and negative. Soil moisture levels in the unsaturated zone directly affect the soil suction and weight. While higher soil suctions during droughts can enhance the soil strength along the slip plane, lighter soils can reduce effective stresses and worsen stability. However, lighter soils can also contribute to a smaller thriving moment, thereby enhancing stability. For hydraulic head levels, the relationship seems to be more straightforward: higher head levels result in less stable dikes, because of higher pore-water pressures and less effective stresses (Ridley et al., 2004). Next to the direct impact on effective stresses, droughts can also induce weakening processes that decrease the soil resistance. It is shown that the hydraulic material properties, including permeability and water retention, are affected by cyclic wetting and drying and are fundamental properties for slope stability (Stirling et al., 2021). Two failed Dutch canal dikes in the summer of 2003 were primarily caused by weight loss and soil shrinkage, due to the dry weather conditions (Bezuijen et al., 2005; Van Baars, 2005). Cracks in canal dikes can also reduce the shear resistance and may lead to the formation of shallow slip planes (Zhang et al., 2021). In the past, dike failures were also attributed to seepage through cracks, caused by the settlement of the dike and due to shrinkage cracks on the dike body caused by exposures (Pigott et al., 1992).

The combination of a higher water level just after a drought can also result in unsafe situations. Deyer et al. (2009) suggest that desiccation can create an interconnected network of cracks that increases the permeability of the fill material and hence allows rapid seepage of flood water through the surface layer of the embankment. When the water level increases after droughts, high rates of seepage may cause localized uplifting of soil blocks, leading to progressive slope failure and successive breaching. Another cascading interaction between dry and wet situations impacting stability is an increased infiltration during extreme precipitation after prolonged drought caused by desiccation cracks in dikes (AghaKouchak et al., 2023; Jamalinia et al., 2020; Shao et al., 2015; Vahedifard et al., 2016; Vardon, 2015). Figure 1 conceptual illustrates the subsurface water conditions within dikes, the influence of various factors on groundwater flow and highlighting the impact of changing soil moisture and head levels on dike stability. The impact of changing subsurface water conditions on stability varies depending on the case. Nonetheless, studying how meteorological conditions affect these subsurface water conditions is the first step in understanding the impact of droughts on dike stability.

2.1.1. The Dutch Situation and Safety Assessments

In the Netherlands, peat dikes consisting predominantly of original in situ peat with a clay cover, spanning about 3,000 km of the canal dikes (Bezuijen et al., 2005), are especially vulnerable to droughts. Variations in the weights of peat soils, an organic soil made up of partially decomposed plant material with a high water content, can
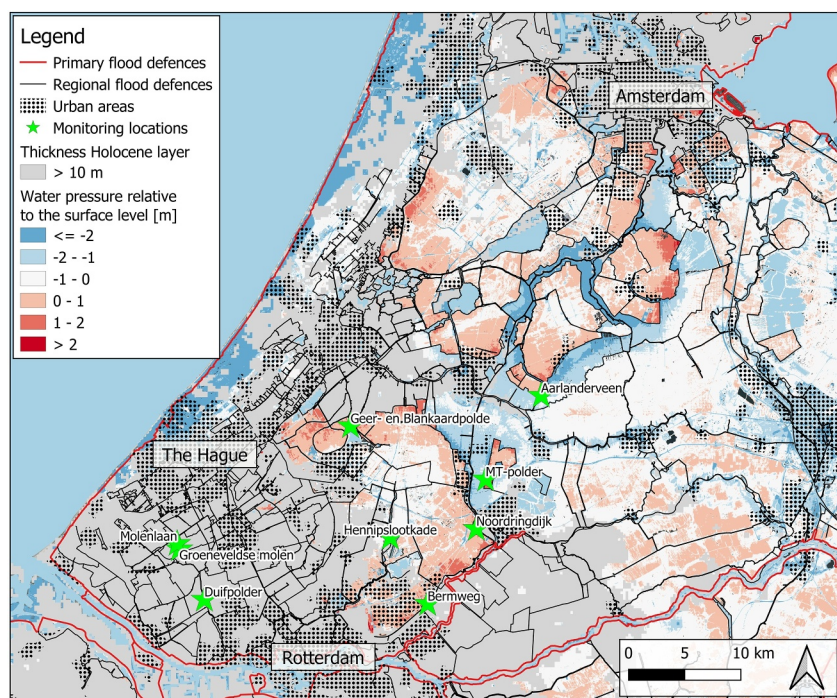
Figure 2. Locations of primary and regional flood defenses in the Western part of the Netherlands are indicated by red and black solid lines. Colors blue to red show the water pressure in the Pleictocene sand layer with regard to the local ground surface elevation (based on data from The Netherlands Hydrological Instrument, De Lange et al. (2014)). Gray areas indicate areas where the Holocene layer is thicker than 10 m and high water pressures in the Pleistocene sand layer supposed to be less relevant for dike safety.

influence the stability, and shrinkage of peat can have large indirect effects on stability, such as causing internal seepage and erosion, and enabling the efficient transfer of high water pressures. Over the past decades, layers of clay have been added to these dikes to maintain an adequate crest height, increase their weight and help prevent the underlying peat soils from drying out. The recent Dutch landscape is formed by Holocene deposits, which are rich in organic matter, on top of Pleistocene sediments (Berendsen & Stouthamer, 2002). Drainage and excavation of peatlands lowered the surface locally and created deep polders with canal dikes situated on top of Holocene deposits. The hydraulic head in the underlying Pleistocene aquifer can exceed the surface (water) levels (Oude Essink et al., 2010), as illustrated in Figure 2. This geohydrological situation can result in marginally stable canal dikes, due to the lightweight peat soils and low effective stresses in soils. The drying of peat soils can be critical for dike stability, and a reduction of 300 mm of water subtracted from the unsaturated zone can lead to dike failures, as demonstrated by Van Baars (2005).

Water authorities assess the safety of canal dikes periodically (every 6 years) to ensure that they meet the required protection levels, which are often based on the acceptable risk of flooding (Vrijling, 2001). In line with the International Levee Handbook (Sharp et al., 2013), the Dutch guidelines prescribe to assess, among others, the failure mechanism of inner-slope instability, where two different loading events are considered: the wet and dry situation. In wet situations, the phreatic surface is close to the surface and soils are fully saturated, while under dry situations the phreatic surface is assumed to be several meters lower and the soil weights in the unsaturated zone are reduced. In both situations, the Mohr-Coulomb constitutive model is used to govern the soil mechanical behavior, assuming drained conditions. In practice, safety assessments indicate that most canal dikes are less stable during wet situations compared to dry situations, because lowering the phreatic surface increases effective stresses and enhances the dike stability, which outweighs the decrease in soil weight. The current safety assessment does account for the effects of fluctuating soil suction levels, swelling and shrinkage and shear-strength reduction, partly due to insufficient data availability. As a result, it may not accurately estimate risks during droughts realistically.

Drought recovery of dikes helps to understand seasonal transitions and the sequence of different failure mechanisms, during dry and wet situations. The geohydrological response to heavy precipitation varies depending on the hydraulic state of the dike. For example, in saturated soils, head levels will increase more than in dried-out soils, where more water can be stored in the unsaturated layers, Furthermore, as droughts are expected to become more frequent (Philip et al., 2020) and the time between droughts may become shorter than the recovery time for certain (ground)water systems, it is important to evaluate the recovery time of droughts. The recovery time is the duration required for a system to return to its pre-drought functional state. This metric is commonly used for ecosystems (Liu et al., 2019; Schwalm et al., 2017), but is also useful for the assessments of dikes. In this study, the drought recovery period is defined as the period between the moment of maximum drought and the moment that the average winter situation, between the beginning of October and the end of March, is reached. The average winter situation is characterized by nearly fully saturated soils, indicating the transition to a different season.

2.2. Drought Indicators

Droughts can typically be classified into three types: meteorological drought (resulting from rainfall deficit), soil moisture drought and hydrological drought (surface and groundwater water deficit) (Hisdal et al., 2001; Lloyd-Hughes, 2014; Van Loon, 2015). These categories can provide a useful framework for understanding the impact of droughts on dike stability. Meteorological drought indicators are often used for drought analysis, as they are easy to calculate and require less data and information compared to other indicators. A meteorological drought can translate into a soil moisture and groundwater drought, as a lack of precipitation and ongoing evaporation can lead to decreasing soil moisture levels and lowering hydraulic head levels. Additionally, there is an interplay between soil moisture in the unsaturated zone and hydraulic head levels, because of the capillary rise of groundwater (when hydraulic head levels are shallow) and soil moisture content levels influence the ability of recharge (Hillel, 2003). Soil moisture droughts and groundwater droughts together form the drought in a dike and influence the stability by means of soil weight, soil suctions, hydraulic head levels and crack formation.
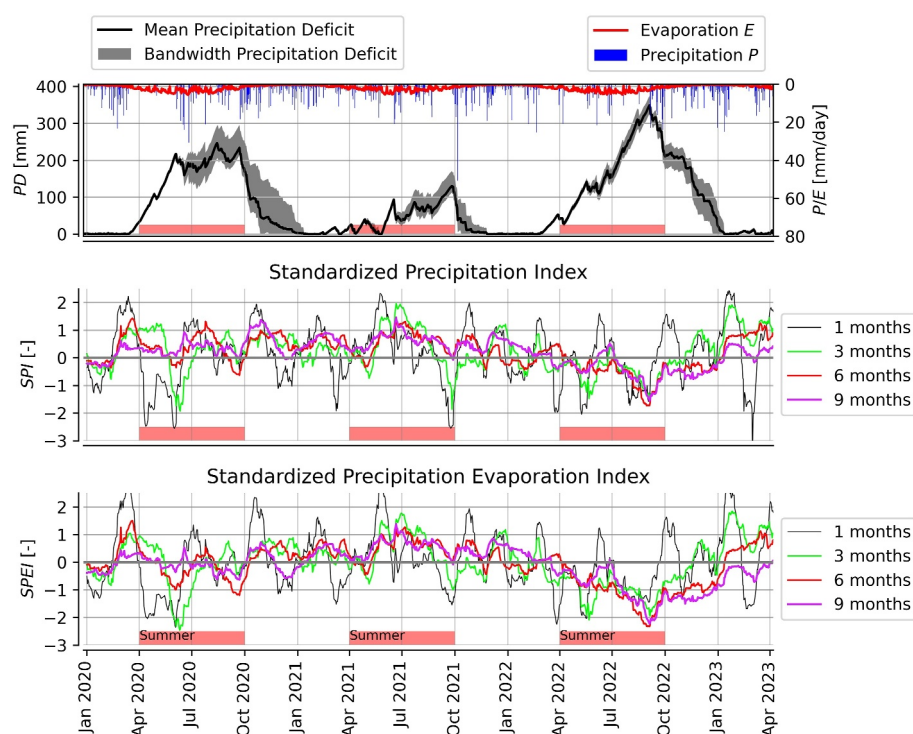
2.2.1. Meteorological Drought Indicators

In order to identify drought periods and compare drought severity between locations, meteorological-based (e.g., rainfall and evaporation) drought indicators are often used, for example, to decide whether inspections of dikes have to start. Meteorological data, such as satellite- and radar-derived precipitation amounts combined with climate and weather models (Muñoz-Sabater et al., 2021), are widely available and cover a long period, making them practical for decision-making purposes. Many meteorological drought indicators are available (Kchouk et al., 2021; Van Loon, 2015) and assess the meteorological and hydrological droughts and their relationships (Senatilleke et al., 2023). Two commonly used meteorological drought indicators are the Standardized Precipitation Index (McKee et al., 1993) and the more extensive Standardized Precipitation and Evaporation Index (Vicente-Serrano et al., 2010), referred to as the *SPI* and *SPEI*, respectively. These indicators measure deviations in rainfall (and evaporation) over a given period (e.g., 2, 6, or 12 months depending on the time scale of interest) compared to the long-term average over the same period. These indicators can be interpreted as the number of standard deviations by which the observed anomaly deviates from the long-term mean. In this study, the *SPI* and *SPEI* were calculated using a gamma and normal distribution transformation, respectively.

Additionally, this study looked at the PD, which is a commonly used meteorological drought indicator in the Netherlands (Van der Wiel et al., 2024). The *PD* is defined as the cumulative difference between precipitation and grass reference evaporation from April 1 onward (the start of the hydrological summer or growing season in the Netherlands). When the *PD* becomes negative, it is reset to zero (Beersma & Buishand, 2004, 2007). It is primarily used for agriculture purposes and similar measures, such as the Soil Moisture Deficit in UK, can be found in other countries (Clark, 2002; Schulte et al., 2005). In this study, the continuous PD at time t (PD_t) is defined as follows, where excess rainfall is fully drained (capped at zero):

$$PD_t = \max\left(PD_{t-1} + E_t - P_t, 0\right)$$

where E is the reference evaporation in mm based on the Makkink formula (De Bruin & Stickler, 2000), which is appropriate for Dutch climate conditions, and P is the amount of precipitation in mm.

Figure 3. Different meteorological drought indicators from January 2020 to November 2022 (measurement period) by averaging values over all monitoring sites. The upper graph shows on the left *y*-axis the precipitation deficit and on the right *y*-axis the precipitation *P* (blue) and potential evaporation *E* (red). The middle and lower graphs show the *SPI* and *SPEI* for different time periods (1, 3, 6 and 9 months), where negative values indicate below-average conditions, suggesting drier or more severe drought conditions compared to the long-term average and positive values indicate above-average conditions.

Meteorological drought indicators can be locally estimated by considering local precipitation and evaporation levels. In this study, RADAR-derived precipitation amounts (Wolters et al., 2013), which have a spatial resolution of 1 km, and triangular interpolation between the estimated grass reference evaporation at KNMI stations are used. The radar-derived product is not available for long-term periods of historical meteorological data to derive standardized indicators. Therefore, the measurements at the KNMI station Rotterdam are used for historical data prior to 1 January 2020, thereby extending the time series back to 1990. The grass reference evaporation, which assumes a well-watered and maintained grass, is used rather than the actual evaporation, which is influenced by vegetation type and plant stresses. Some models can take into account factors like drainage, soil type and vegetation (Schulte et al., 2005), but additional information about these factors is often not present and for dike safety purposes barely used.

Figure 3 illustrates the development of the considered meteorological drought indicators by averaging values over all monitoring sites. In the summers of 2020 and 2022, the average maximum precipitation deficits were approximately 250 and 350 mm, corresponding to an exceedance probability of 1/15 and 1/60 per year (Beersma & Buishand, 2007). The *SPEI* aggregated over three months indicates extremely dry summers ($SPEI < -2$) for 2020 and 2022, while aggregating over 6-month period results in extremely dry summers in 2022 and a moderate drought ($-1.5 < SPEI < -1$) in the summer of 2020. The thresholds to identify droughts of dikes and prompt inspections depend on the susceptibility of the dikes to droughts, which is dike-specific and can range from minimal to substantial impact on dike stability. Commonly used thresholds for identifying droughts and initiating inspections include a threshold of -1 for *SPI/SPEI* (McKee et al., 1993) and a *PD* of approximately 175 mm, following common practices in the Netherlands, which is typically exceeded every 3 years (Beersma & Buishand, 2007). This study connects meteorological drought indicators with subsurface water conditions, and a subsequent step could involve quantifying their impact on stability to enhance the substantiation of thresholds.

3. Monitoring Sites

3.1. Dike Characteristics

The monitoring network consists of 10 locations where subsurface water conditions of canal dikes are measured (see Figure 2) from February 2020 to March 2023 (Strijker, 2023). These dikes are the result of historic human activities and primarily consist of various clays (silty and sandy clays with different levels of organic matter) and peats, with occasional thin layers of sand and gravel. Additionally, remnants of human activities, such as fragments of pots and glass, as well as metal objects, were found in the dikes. This makes the composition of the dikes rather heterogeneous, making it challenging to model and predict flow paths.

Under normal conditions, where excessive precipitation events are absent, the water levels in the canals remain constant, but the levels can increase by several tens of centimeters during heavy precipitation. The characteristics of these dikes differ, like head difference, dimensions and subsoil characteristics. The cross-sectional profiles and classified soil properties of the boreholes are shown in Figure 4. The degree of organic matter (moderate or high) in clay is high for all locations (peat contains by definition a large amount of organic matter). Based on soil properties, a distinction can be made between dikes where the dike body mainly consists of clay material (nr 1–4) and peat material (nr 5–10). Note that the peat dikes are not solely composed of peat; clay layers are often present, including a clay cover on top. The dike bodies at all the monitoring sites are located on Dutch Holocene deposits. The thickness of the Holocene deposits, which consist of clay, silt or peat, varies and shows a west- and northward thickening in the Netherlands (van der Meulen et al., 2007), resulting in an approximately 5m thick Holocene layer at Aarlanderveen and the MT-polder and about 15m at the Duifpolder (Table 1 shows the top of the Pleistocene layer w.r.t. The national reference level NAP).

In this paper, a distinction is made between monitoring sites and monitoring points. There are 10 monitoring sites, comprising four or five monitoring points each. These points are positioned in a cross-sectional profile of the dike at which soil moisture levels (at different depths) and/or the hydraulic head level is measured. The dikes are all vegetation-covered with varying species that can have plant material above the ground surface up to 50 cm. The Noordringdijk includes a road construction near the toe of the dike, while the Hennipslootkade features a small asphalt cycle path along its crest. Other locations do not have any road constructions.

Soil samples from different monitoring points and depths are taken and analyzed in the laboratory to determine the in-situ and dry volumetric weight, in-situ water content, soil particle distribution by sieving (>63 μm) and sedimentation techniques (<63 μm) and organic matter. The soil samples were mainly taken up to 2 m below the ground surface, as they were used to interpret the soils where soil moisture sensors were installed (next paragraph). These data are available in Strijker (2023).

3.2. Monitoring Equipment

The measured variables are the volumetric soil moisture content levels and the hydraulic head levels. The general set-up of the monitoring equipment can be seen in Figure 5, where five standpipes are installed within a cross-sectional profile and next to them the soil moisture sensors are installed at several depths. There are no soil moisture sensors installed next to standpipe P5, since fluctuations of the soil moisture are low due to (expected) high hydraulic head levels. At several locations, a conscious decision has been made to deviate from the general set-up, because there was not enough space to install five standpipes or the soil moisture sensors could not be placed because of the subsoil conditions (e.g., gravel layers). Table 2 shows the monitoring equipment used.

3.2.1. Soil Moisture Content

TEROS 11 and TEROS 12 sensors from METER Group were used to measure the soil moisture and soil temperature (TEROS 11/12) and the electrical conductivity (TEROS12 only). The majority of sensors utilized were TEROS11, with TEROS12 sensors specifically placed in the dike crest. This placement was chosen due to the greater depth of the water table compared to the surface level, where cracks are more likely to occur. The formation of cracks can affect the evolution of the electrical conductivity (Kong et al., 2012), potentially providing valuable insights when electrical conductivity was measured. However, no significant cracks were observed at the monitoring sites. The TEROS 11/12 determines the soil moisture content levels using capacitance/frequency-domain technology. It uses an electromagnetic field between two metal electrodes (probes or needles) to measure the dielectric permittivity of the surrounding medium. The measurement sensitivity is contained within a 1.010-
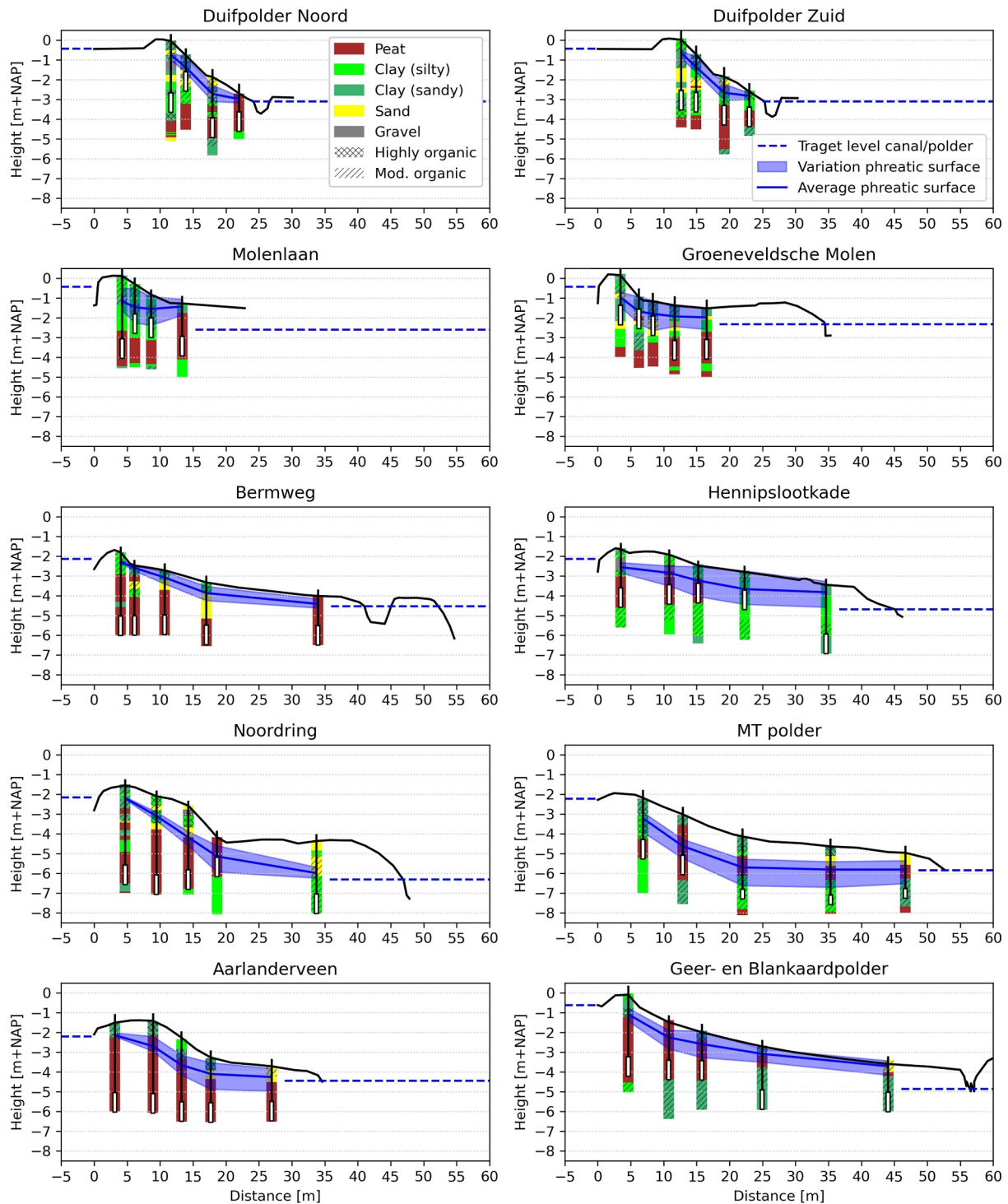
Figure 4. Cross-sectional profiles of monitoring sites. Solid black lines indicate the ground surface level and the dashed blue lines indicate the target water level in the canal and polder or ditch. Within every cross-sectional profile, boreholes are shown where colors indicate soil types and the vertical black line ending with a white rectangular box indicates the standpipes. The blue areas show the variation of the hydraulic head levels based on the highest and lowest measured hydraulic heads at the standpipes and represent the phreatic surface through the dike.

mL volume and the sensor uses a 70-MHz frequency that minimizes the salinity and textural effects. These sensors were not individually calibrated and the standard calibration curve is used that gives an absolute accuracy of ± 0.03 m^3/m^3 for most mineral soils (Meter Group, 2021). The standard calibration curve was used for

Table 1
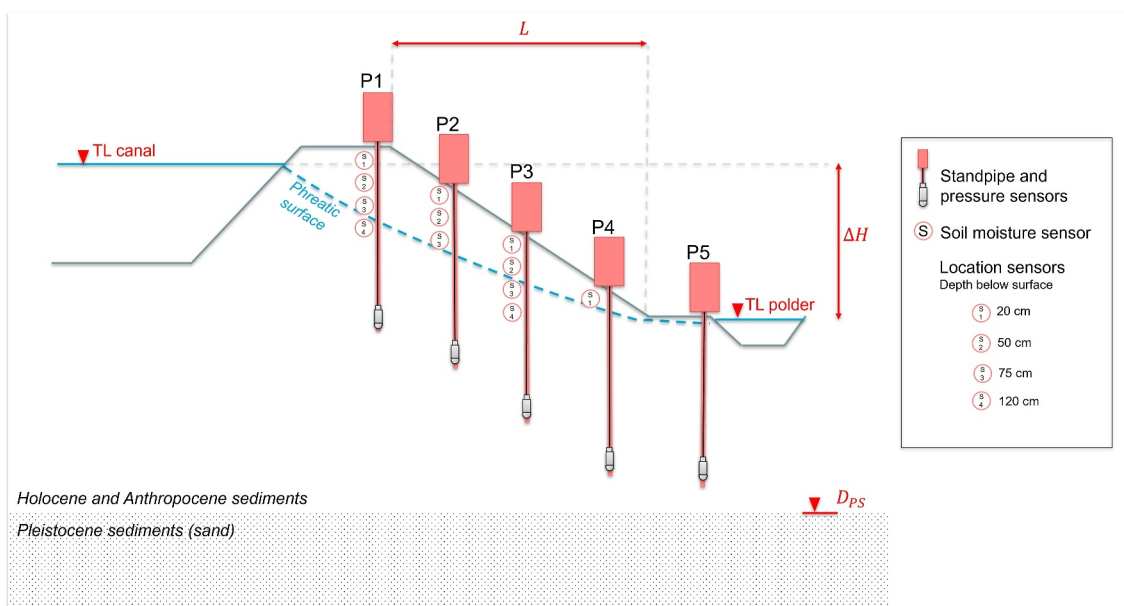*Characteristics of the Monitoring Sites (See Figure 2 for Geographic Locations)*

Nr	Location name	TL canal [m + NAP]	TL polder [m + NAP]	ΔH [m]	L [m]	$\Delta H/ L$	β [°]	D_{PS} [m + NAP]	Distance first piezometer to canal [m]	Distance last piezometer to ditch [m]
1	Duifpolder Noord	−0.43	−3.10	2.67	12.5	0.21	255	−19.5	4.1	2.2
2	Duifpolder Zuid	−0.43	−3.10	2.67	12.5	0.21	255	−19.5	4.1	2.3
3	Groeneveldse-Molen	−0.43	−2.32	1.89	31	0.06	245	−21.5	3.3	18.0
4	Molenlaan	−0.43	−2.60	2.17	–	–	65	−21.0	3.7	–
5	Bermweg	−2.15	−4.55	2.4	37.0	0.06	320	−12.5	3.0	7.0
6	Hennipslootkade	−2.15	−4.70	2.55	36.5	0.07	130	−12.5	3.0	9.9
7	Noordringdijk	−2.15	−6.32	4.17	40.5	0.10	225	−13.5	3.9	13.2
8	MT-polder	−2.29	−5.84	3.55	44.5	0.08	105	−11.0	7.2	6.0
9	Aarlanderveen	−2.25	−4.44	2.19	25.5	0.09	295	−9.5	3.1	7.7
10	Geer-& Blankaardpolder	−0.61	−4.86	4.25	50.5	0.08	325	−13.0	4.6	12.5

Note. The reference level is NAP: Normaal Amsterdams Peil. TL = Target water level, ΔH = head difference between canal and polder, L = distance between inner crest and toe, β = orientation of the dike relative to the North, D_{PS} = the depth of the Pleistocene sand layer. The symbols are conceptually illustrated in Figure 5.

efficiency reasons, as individually calibrating all 120 sensors would be time-consuming and costly, while ensuring consistency in measurements across the locations. The sensor readings were recorded at 60-min intervals. The timezone was aligned with the local timezone and differs for the summer (UTC+2) and winter (UTC+1). These sensors were connected to a ZENTRA (ZL6) data logger by Meter group and sent the data every day to the data platform ZENTRA Cloud.

3.2.2. Hydraulic Head Levels

Hydraulic head levels were measured in standpipes, also known as open standpipe piezometers, that were placed at several locations within the dike body. The diameter of the installed standpipes and filters are both 32 mm. Filter gravels were placed around the filters and on top a bentonite cement grout of 100 cm (and at some locations 50 cm) was used to prevent groundwater flow from other soil layers. The standpipes were sealed around with

Figure 5. Schematic overview of the general set-up of the monitoring equipment. This cross-section also includes various definitions (in red) of the dike characteristics, as stated in Table 1.

Table 2
Overview of Sensors That Were Used to Measure Certain Variables

Sensor	Variable	Unit
TEROS-11/12	Soil moisture content (11/12)	$[m^3/m^3]$
	Soil temperature (11/12)	[degrees Celsius]
	Electrical conductivity (12)	[mS/cm]
TD-Diver	Hydraulic head level	[cm H_2O]

Note. Numbers between brackets behind variables that are measured by the TEROS sensors indicate the model; soil electrical conductivity was only measured by TEROS-12 sensor, while soil moisture content and soil temperature were measured by both TEROS-11 and TEROS-12.

swelling clay. The standpipes were equipped with TD-divers (DI801) that measure the pressure. The accuracy of the TD-diver used is 0.5 cm H_2O water column and can measure the water column up to 10 m (Van Essen, 2016). The sensor readings were collected at hourly intervals.

In low hydraulic conductivity materials, like heavy clay soils with a clay percentage of more than 50%, there is often disequilibrium between the head in the pipe and the head in the surrounding soil layer (Neuzil, 1986; Wolff & Olsen, 1968). Groundwater flow through low permeability layers can be slow and it may take hours to weeks for enough water to flow through the medium near the pervious section to establish equivalent heads in the pipe and the medium. Therefore, the measurements of the water level in the piezometer pipe may be subject to attenuation and time lags. An alternative is to use a pressure transducer that needs a smaller water quantity to obtain a measurement and gives a faster response time for measuring head level variations. For the purpose of this study, 18 pressure transducers were deployed at four distinct monitoring sites. However, it was determined that a majority (90%) of these sensors provided inaccurate and unrealistic data. As a result, standpipes were utilized as an alternative method for obtaining long-term monitoring data. The reason for this discrepancy remains unknown and requires further investigation. Nevertheless, the observed head levels demonstrate a flashy and reactive behavior, suggesting limited attenuation and damping, see Figure 7. The head response following a heavy rainfall event exhibits rapid peak reactions the day after. Moreover, given the focus of this study on droughts, where head level changes are generally slower, the influence of standpipes can be anticipated to be minimal.

3.3. Subsurface Water Measures for Dikes

The volumetric soil moisture content is the volume of water within a total soil volume and it varies at different depths. For dike safety purposes, the total amount of soil moisture in a soil column is relevant (Van Baars, 2005) rather than a point measurement at one depth. Therefore, a measure that represents the integrated soil moisture in a soil column during droughts is introduced, called the Water Storage Capability (*WSC*). This measure gives the amount of water per unit surface area (in mm) that the soil surface absorbs before further precipitation cannot be stored in the profile (i.e., the soil has reached saturation level). The higher the number, the dryer the soil. While a lysimeter can measure the total moisture extraction of a soil column, in many cases, this must be estimated using point measurements that are integrated over the depth. Depending on the thickness of the unsaturated zone and available measurements, different soil column heights can be considered for the *WSC*. The saturation levels are not always known, unless soil samples are analyzed in the laboratory. However, with long-term measurements and information from piezometers indicating shallow head levels close to the surface in winter, it can be assumed that soil moisture levels in winter will approximate saturation levels. Consequently, the maximum measured soil moisture content at various depths can be regarded as an approximation of the saturation level.

In our case, the *WSC* was estimated up to about 1 m below the surface (87.5 cm) by making use of the soil moisture sensors at 20, 50 and 75 cm depth. This integration depth captures most of the dynamics within the unsaturated zone of the dikes, as the majority of soil moisture fluctuations in the dikes occur within the upper meter of the dike, as can be seen in Figures S3, S4 and S5 in Supporting Information S1. Figure 6 illustrates how the *WSC* can be calculated from the in-situ volumetric water content measurements. A simple depth integration is applied and the use of water retention curves may give more accurate estimates of soil moisture profiles and absolute *WSC* levels. Given the application of dike safety and the unknown matric suction profile, the *WSC* measure seems to be reasonable. The time series of the *WSC* for each location is calculated by averaging the *WSC* at the monitoring points where soil moisture levels are measured at depths of 20, 50, and 75 cm. This approach is adopted because the focus is primarily on the drying-out processes of the entire dike, rather than at a specific position in the cross-sectional profile. By averaging data from multiple sensors at different positions in the cross-sectional profile, sensitivity to uncertainties due to spatial variability (resulting from different soil types) and measurement errors linked to individual sensors is reduced. The sensors are uncalibrated, which may result in consistent overestimations or underestimations of actual soil moisture levels, thereby impacting the WSC calculation. However, these systematic uncertainties do not affect the relative development of the WSC and, consequently, the drought development.
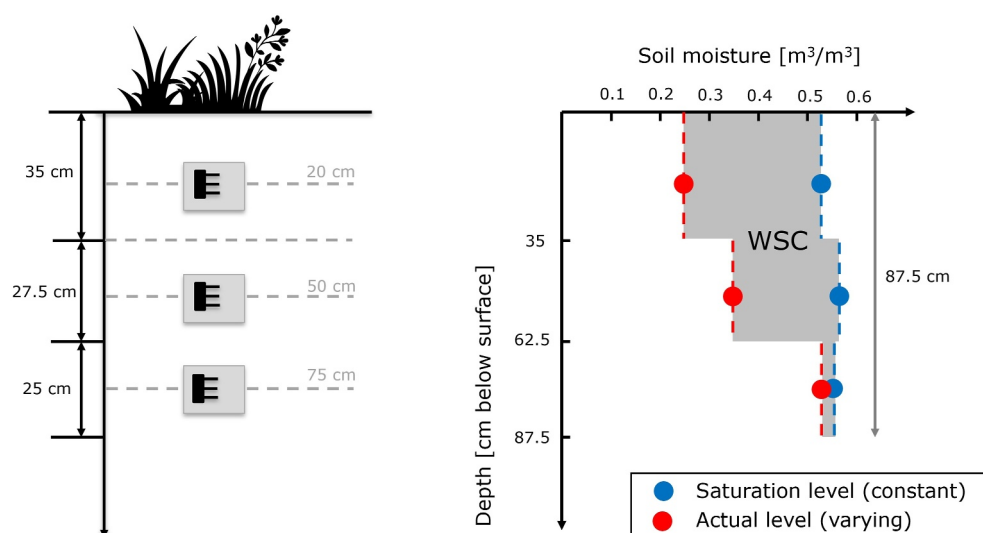
Figure 6. Conceptual illustration of how the water storage capacity (WSC) is calculated. Left drawing shows the different sensor depths and representative soil columns of every sensor. Right drawing shows how the *WSC* is calculated by showing actual soil moisture levels that can vary in time (red) and the saturation level that can be seen as a reference level which is constant and based on the maximum measured soil moisture levels. The volumetric water content does not necessarily increase with depth due to variations in soil types.

4. Results

4.1. Hydraulic Head Observations

Time series of measured hydraulic heads at all monitoring sites, as shown in Figure 7, illustrate the seasonal pattern with high head levels in the winter (October until March) and lower head levels in summer (April until September). The absolute hydraulic head levels, the manner in which head levels decrease during droughts and the responsiveness during heavy rainfall events vary by location. For example, a high responsiveness of heads to a heavy rainfall event in February 2022 with head increases of up to 50 cm at Hennipslootkade or Noordring (upper right graph in Figure 7), while heads at Aarlanderveen, Bermweg and Geer-en Blankaardpolder show limited increases (daily local rainfall amounts ranged from 30 to 50 mm between 19 and 21 February). This can be attributed to the presence of more peaty material in the subsoil at these locations with lower vertical hydraulic conductivity causing different geohydrological responses. During the summer of 2022, a gradual decrease in head levels of approximately 10 cm per week is observed (lower right graph in Figure 7). Despite these fluctuations during drought and heavy rainfall events, the water levels in the canals remain relatively constant, with fluctuations on the order of centimeters. This substantiates that the response of groundwater levels in dikes is primarily driven by meteorological variations.

By analyzing the frequency distributions of measured hydraulic heads using violin plots, some basic characteristics of the groundwater behavior can be extracted (see Figure S1 in Supporting Information S1). At Duifpolder and Bermweg, the tail of the frequency distribution describing the lower head levels is more or less bounded indicating a limit to low head levels. At other locations, like MT-polder, Hennipslootkade and Geer-& Blankaardpolder the tail of lower head levels is long, indicating dropping head levels during the measurement period. Furthermore, upper boundedness can be noticed, for example, at MT polder and Bermweg, where the tail of high head levels is small. At 50% of the monitoring points near the inner slope and toe (position 2 and higher), the maximum hydraulic head levels exceed 0.2 m below the surface within the 3 years measuring period. In these situations, infiltration can be limited during more severe rainfall events as the dike is almost fully saturated, leading to increased surface runoff. This indicates an upper limit to the loading conditions of dikes, which can be relevant for the stability and failure probability of these dikes.

The measured head ranges are linked to the distance between the measurement point and the nearest drainage (canal or ditch), with higher fluctuations observed at greater distances (see Figure S2 in Supporting Information S1). Therefore, wider dikes with a greater distance between the canal and ditch are expected to experience
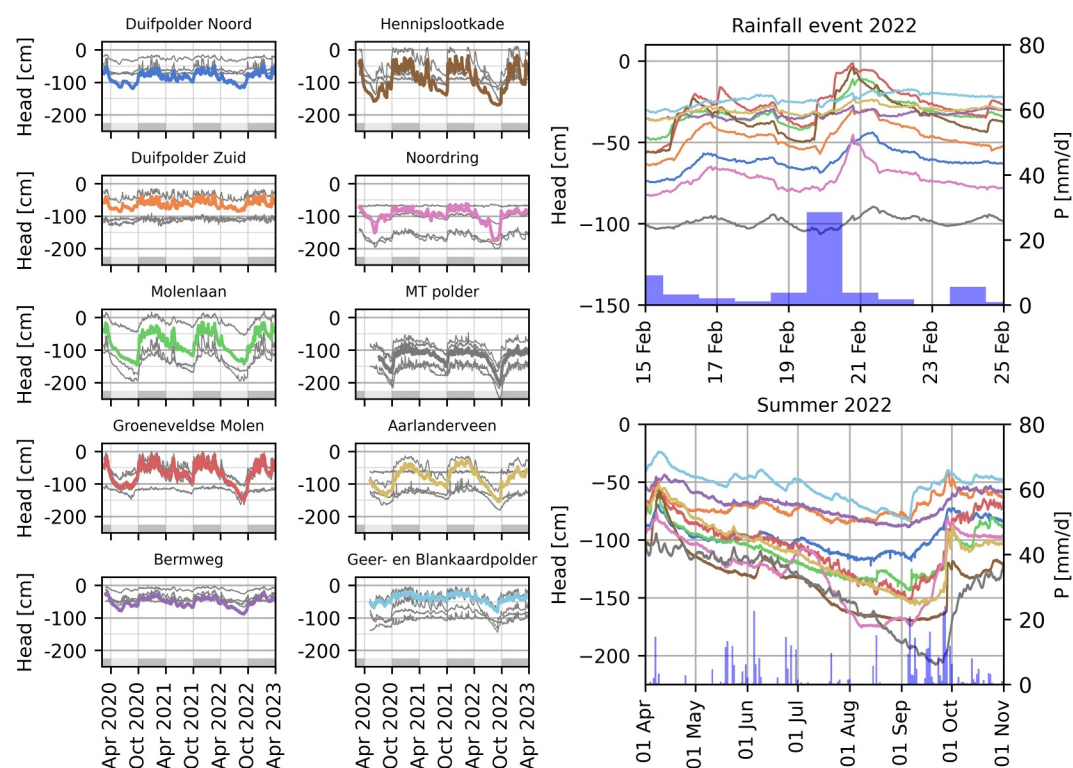
Figure 7. Small graphs on the left show time series of hydraulic head levels at the monitoring sites, where colored lines indicate the representative monitoring point at every location and the gray lines are the monitoring points at other positions within the cross-sectional profile. The representative monitoring point is number three in the cross-sectional profile where the standpipe is located in the inner slope. This monitoring point represents the fluctuations occurring well and is relevant for stability issues. Right: Head levels zoomed in at two events, namely a heavy rainfall event in 2022 (top) and the dry summer in 2022 (below), where the average precipitation and precipitation deficit of all sites is shown.

more head fluctuations than smaller dikes, due to a smaller head gradient and reduced seepage through the dike, coupled with decreased drainage of rainfall. However, this relationship remains ambiguous, and cannot be solely explained by soil type or geometry, even though these factors are expected to be significant, for example, according to Hooghoudt's equation (Hooghoudt, 1940). The heterogeneity of dikes and the resulting unknown flow paths and field hydraulic conductivities may contribute to the unpredictability of the geohydrological response.

4.2. Non-Hydrostatic Hydraulic Head Levels

In most safety assessments of dikes, the primary focus is on high-water events that increase hydraulic head levels or pore-water pressures, including non-hydrostatic heads within the dike, which can lead to failure (TAW, 2004; U.S. Army Corps of Engineers, 2003). For canal dikes, the hydraulic head levels in the dike body during droughts vary with meteorological conditions, and the way this is schematized in safety assessments for drought situations can be crucial for their stability. These head levels within the canal dike body are often assumed to be hydrostatic (Lendering, 2018), or they are linearly interpolated between the phreatic surface and the head in the underlying aquifer. This assumption is often made due to a lack of information about the vertical head profile. Additionally, hydrostatic pressure is relatively easy to incorporate in stability analyses. However, during dry summers, high hydraulic head levels in deeper layers and drying top layers (decreasing soil weights) can lead to severe stability issues for the dike. Time-dependent processes can result in non-hydrostatic head levels and unfavorable conditions for dike stability. At some monitoring points, two piezometers were installed in different soil layers, about 1.5 and 2.0 m vertically apart. The hydraulic heads in the dike body are non-hydrostatic during summers (see Figure 8), causing an upward flow that replenishes the soil moisture depleted by evaporation and root water uptake. In the summer, the head levels in deeper soil layers are up to 50 cm higher compared to shallow layers, whereas in the winter, the head levels tend to approach hydrostatic conditions, where the head levels approach each other. This could have implications for dike stability, because, in this scenario, the effective stresses within
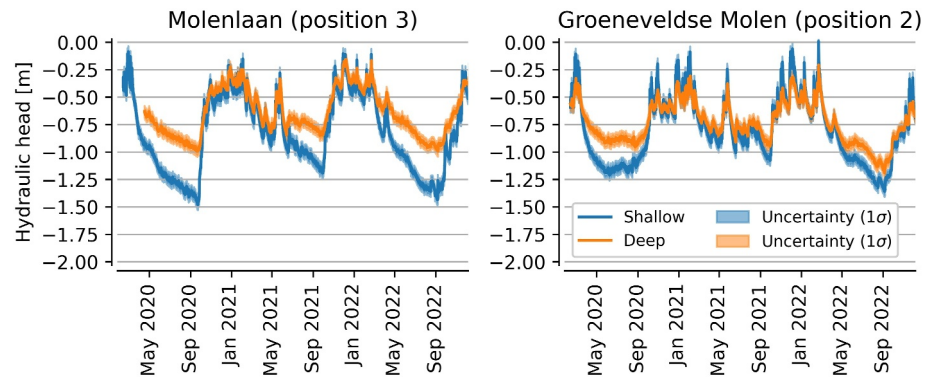
Figure 8. The hydraulic head levels at standpipes that are located at different depths for two monitoring sites. The filter depths (bottom of the filter) in meters below surface level are 2.1/3.45 m (shallow/deep) at Molenlaan and 2.55/4.65 m (shallow/ deep) at Groeneveldse Molen.

the dike can be lower than initially accounted for, due to the remaining high head levels and a reduced soil weight as a result of drying out.

4.3. Drying of Unsaturated Soils

During winter, the unsaturated soils are close to saturation with high groundwater levels and drying occurs during spring and summer, as can be seen by the development of the *WSC* in Figure 9. The decrease in soil moisture levels in the canal dikes is caused by water extraction from the soil by evaporation and transpiration and dropping groundwater levels, but can be replenished by upward capillary flow from the groundwater. The balance between these processes differs for every location. For example, the *WSC* at the Bermweg remains relatively low during all three summers, caused by high groundwater levels that are capable of supplying the unsaturated soils opposing drying from the surface.

The dry summer of 2022 led to dropping soil moisture levels with maximum *WSC* ranging from 65 mm at Bermweg to 153 mm at MT-polder. The summer of 2021 was meteorologically wetter (with a three times smaller average PD than in 2022) and resulted in a larger variation in maximum *WSC* among the monitoring sites compared to 2022. Despite 2022 being meteorologically wetter, the differences in maximum *WSC* between the summers were small at Aarlanderveen and MT-polder, two peat dikes (Aarlanderveen: 122 mm in 2021 and 138 mm in 2022; MT-polder: 111 mm in 2021 and 153 mm in 2022). This demonstrates the significance of
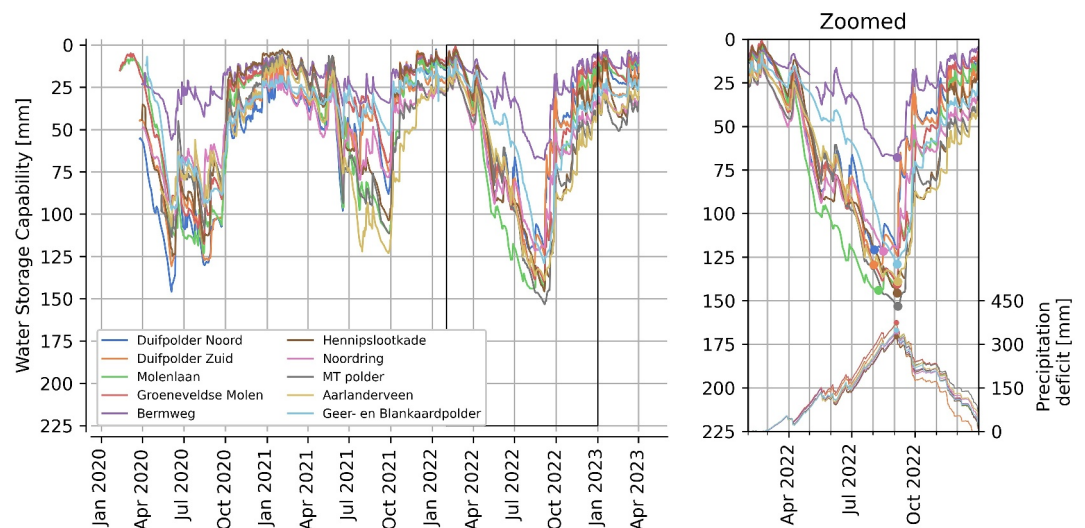

Figure 9. *WSC* during the period 2020–2023. The black box in the left graph indicates the zoomed period in the right graph, where the precipitation deficits are also indicated. The points in the right graph mark the maximum *WSC* and PD.

groundwater flow in dikes and its impact on infiltration, evaporation, and water distribution within the dike, which can result in different severities of drought from meteorological and soil moisture perspectives. An explanation of the two deviating peat dikes can be the hydrophobic property of peaty materials that can block infiltration (Dekker & Ritsema, 2000) or limited groundwater flow through dry, unsaturated soils with very low hydraulic conductivities (Hillel, 2003).

4.4. Relationship Between Soil Moisture and Hydraulic Head

Soil moisture is strongly linked to the water table in the dike due to capillary rise. The relationship between the soil moisture in the unsaturated zone and hydraulic head levels deeper in the dike is crucial to understand the joint impact of both states on dike stability. Moreover, these relationships are also useful for dike monitoring; soil moisture levels can be measured during inspections, and remote sensing techniques are available that observe soil moisture levels in dikes (Aanstoos et al., 2011; Cundill, 2016). The conditions of soil moisture and water table, and their interactions, are not static but dynamic and influenced by time-dependent changes in environmental conditions (e.g., rainfall and the evaporative demand of the atmosphere) and the storage capacity and transmissivity of soils. On top of this, there is also the effect of hysteresis where the water content—hydraulic head relationship follow state dependent different paths for the wetting and drying cycles. In general, unsaturated soils dry out at the surface due to evapotranspiration, and when the water table is shallow, upward capillary flow can replenish the drying soils when the hydraulic conductivity of the soil is large enough. However, the water table in canal dikes itself is also dynamic and affected by the hydraulic resistance of the dike and seepage from deeper soil layers. This complexity adds challenges to data analysis when studying the interactions with soil moisture. Whether a soil profile is dominated by capillary rise can be investigated by considering the soil moisture levels at a specific depth in relation to the height above the water table (see Figure 10). In cases where capillary rise governs the soil profile, the moisture levels tend to exhibit a relatively small range of variation in relation to the water table height. At Aarlanderveen, the range of soil moisture is narrow at small heights above the water table and widens as the height increases. This suggests the presence of sufficient capillary rise near the water table, while evaporative demand becomes more dominant closer to the surface. Influences of the capillary rise can also be noticed at Noordring, Bermweg and Duifpolder Noord. At other locations, the range of soil moisture is wide, indicating a dominant influence of the evaporative demand at the surface, for example, at Molenlaan and MT-
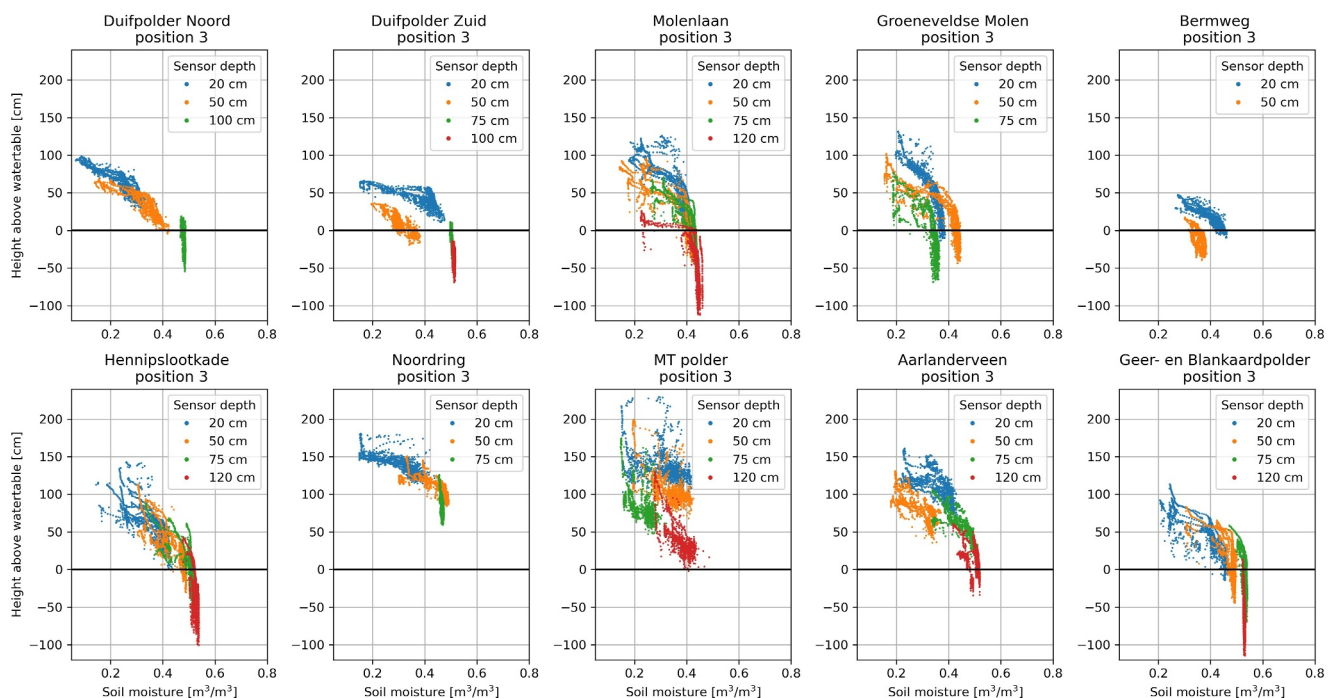

Figure 10. Measured moisture content levels plotted (*x*-axis) against the sensor height relative to the groundwater level (*y*-axis) for different soil moisture sensors at 3rd monitoring point in the cross-sections.

polder. Saturated soil moisture levels (moisture values below the water table) exhibit variations, such as Geer&Blankaard, Bermweg, and Groeneveldse molen. These variations can be explained by changes in soil volume resulting from soil compaction caused by changes in effective stresses (see also Figures S3–S5 in Supporting Information S1) or non-hydrostatic hydraulic head levels, which can cause the actual water table to be lower and the soils to be unsaturated.

4.5. Applicability of Meteorological Drought Indicators for Dikes

For dike stability, the development of the absolute level of hydraulic head and soil moisture are of main interest and are used as target measures in this analysis. Three types of meteorological indicators were assessed: the PD and the standardized indicators, *SPEI* and *SPI*, for different timescales (1, 2, 3, 6 and 9 months). The relationships between these meteorological drought indicators and subsurface water measures (hydraulic head level at the inner slope and *WSC*) are evaluated using the adjusted *R*-squared of a second-order polynomial regression and the Pearson correlation coefficient and the Spearman rank correlation (Wright, 1921). The relationships are assessed for every individual location for the summer period, from April until September. In this section, the results presented using the adjusted *R*-squared, with the Pearson correlation coefficient and the Spearman rank correlation are only reported, Figures S6 and S7 in Supporting Information S1, and yield similar findings.

The PD performs as the best meteorological drought indicator to assess the dryness of subsurface water conditions in nearly all canal dikes considered, see Figure 11. In general, it provides significantly better estimates of subsurface water conditions during droughts than the standardized indicators. Precipitation (or its absence) and evaporation are the primary atmospheric processes directly linked to soil moisture fluctuations, which makes the *PD* emerges as the top performer among the indicators for the *WSC*. However, certain factors such as percolation, capillary rise, surface runoff, and soil moisture redistribution are not considered by the *PD* and could contribute to discrepancies in its performance across different dikes. Since groundwater levels in dikes are shallow and react quickly to changes, often within a day, this rapid response contributes to the effectiveness of the PD. At two locations, the *SPEI-6* proved to be a more effective indicator for groundwater drought. In one location, head level fluctuations are generally minimal, likely due to significant influence from horizontal seepage from the canal. An advantage of the *PD*, in relation to standardized indices, is that you do not need to select a specific time frame, making the application of this drought indicator easier. The standardized indicators have limitations in estimating
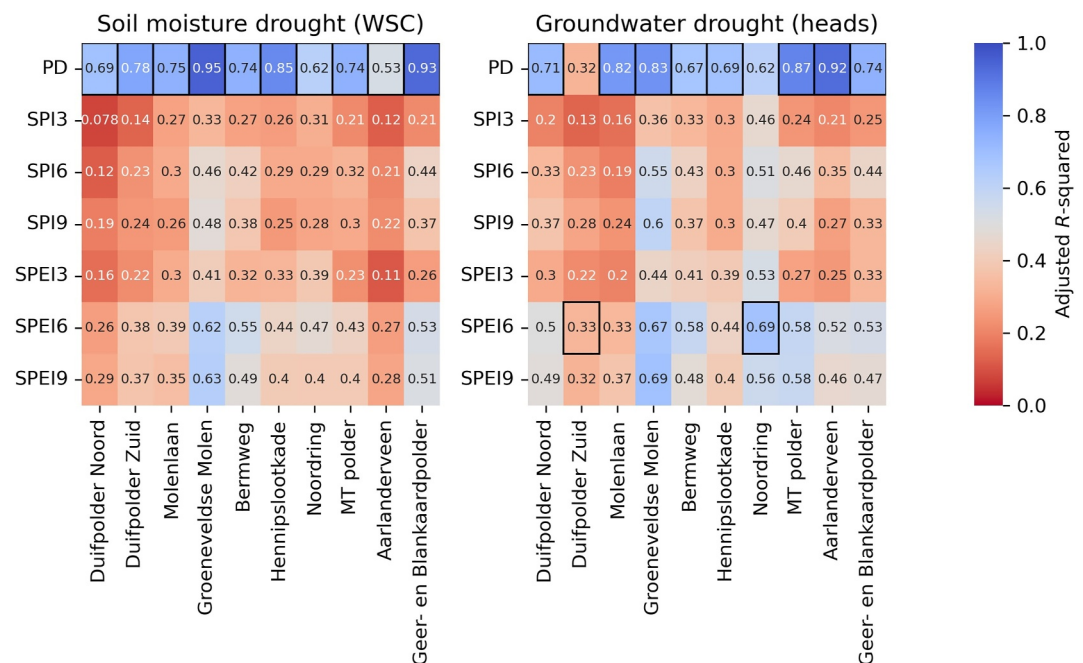

Figure 11. Relationship between different meteorological drought indicators and subsurface water measurements in dikes was evaluated using the adjusted *R*-squared. Values in the heatmap are the adjusted *R*-squared of the polynomial regression: higher values indicate a better fit than lower values.

the absolute subsurface water conditions, as they filter out seasonality and express droughts in relative terms. Furthermore, it can be seen that the evaporation term is crucial for the subsurface water conditions, both for soil moisture deficit and groundwater levels, as the *SPEI* generally shows a better fit than the *SPI*. Figures S8–S11 in Supporting Information S1 provide a more detailed view of the relationship between the two most effective meteorological drought indicators (*PD* and *SPEI-6*) and the subsurface water measures.

Although the PD is the most effective meteorological drought index, the absolute severity of droughts in dikes varies strongly. Therefore, these indicators provide information about the dryness at each location in relative terms, while the absolute subsurface water conditions depend on other local dike characteristics. Furthermore, the *WSC* measure is limited to the soil moisture in the upper meter of the dike. For a high PD, the amount of soil moisture extracted may extend to deeper soil layers, which are not included in the *WSC*. As a result, the *WSC* may reach a maximum value contributing to the fitted polynomial model that is concave down at eight locations. However, another factor that can also impact this trend is the prolonged duration of drought. During prolonged droughts, the evaporation rate can be limited or dictated by the rate at which the gradually drying soil profile can supply moisture to the evaporation zone, as the hydraulic conductivity of dried soils decreases (Hillel, 2003). At the locations Bermweg and Geer&-Blankaardpolder, the fitted polynomial model is concave up, which can be explained by the interaction with the head levels: at the beginning of the dry periods, high heads kept the *WSC* small, but later on, as head levels dropped, the soils still dry out.

4.6. Drought Recovery

The moment of maximum drought (start time of recovery period) and recovery moment (end time of recovery period) were calculated for different concepts of drought (meteorological, soil moisture and groundwater). These moments vary by location and drought concept, as shown in Figure 12. For most locations, the recovery moment for the soil moisture drought occurs later than for the groundwater drought, as can be seen during summers in 2020 and 2022. This is different compared to other systems, like river catchments (Van Loon, 2015), and can be caused by different storage characteristics. The soil moisture and groundwater recovery following the exceptionally dry summer of 2022 took up to 4.5 months across various locations and drought recovery occurred in January next year. This exceeded the onset of the subsequent storm/winter season. Despite heavy precipitation events in the winter, the previously dried soils were able to effectively store the water, thus mitigating potential high hydraulic head levels and instabilities. Furthermore, the maximum and recovery moment of the PD, representing the meteorological drought, are indicated in Figure 12, which differ from the subsurface water conditions. These differences can be caused by physical elements affecting the infiltration, total evaporation and water redistribution within the dike that are not accounted for in the PD.
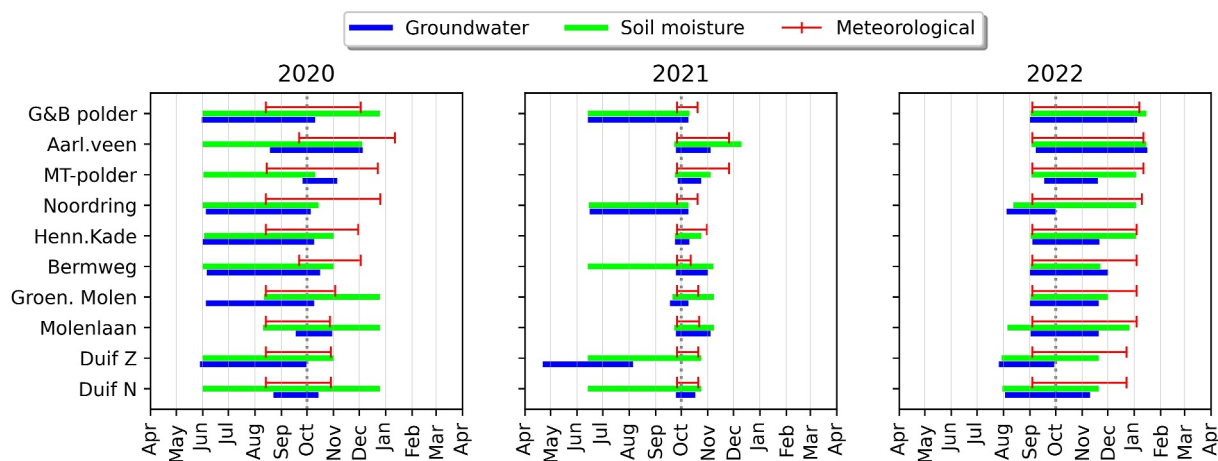
Figure 12. Horizontal bars indicate the recovery period, which is defined as the difference between the moment that maximum drought (highest *WSC* or lowest hydraulic head level) occurs and the moment of recovery. Vertical red markers indicate the moment of maximum drought and recovery moment based on the continuous rainfall deficit (meteorological drought). The gray dotted line indicates the start of the storm/winter season. During this period there are high probabilities of hydraulic loads.

5. Discussion

5.1. Limitations

The data set comprises 10 monitoring sites, which is unique in the Netherlands, but statistically insignificant given the large heterogeneity of canal dikes. While the data set includes some typical canal dikes, such as peat dikes with gentle slopes that are common in the Netherlands, its representativeness for the geohydrological response remains uncertain, primarily due to limited multi-year observations in general. The accuracy of the soil moisture measurements requires attention since the factory calibration equation is used, which can be improved by a custom calibration. Furthermore, attenuation and time lags can occur when measuring head levels in standpipes that are placed in soils with low hydraulic conductivity levels, like clay and peat.

In addition, it is important to consider that it is assumed that several point measurements of soil moisture levels together represent the state of a certain dike. However, uneven wetting and preferential flow paths, caused by burrowing animals, plant roots or cracks, can make the point measurements unrepresentative. Next, the applicability of meteorological drought indicators for dikes has been assessed based on absolute values of soil moisture and groundwater levels. In this case, standardized indicators may not perform as well, but when one is interested in how dry a dike is at a certain moment compared to previous years, standardized meteorological indicators may be more suitable. Lastly, the definition of drought recovery is an assumption in this study, considering the period between the maximum drought and the average winter situation. This choice is based on the application to dikes with two failure mechanisms in summer and winter. However, drought recovery can also be defined differently which can give different outcomes.

5.2. Implications

Currently, nearly all inspections by Dutch water authorities are conducted visually, with other methods used occasionally or in the early development phase, like deformation data using satellite radar interferometry and ground penetrating radar (Chlaib et al., 2014; Özer, Rikkert, et al., 2019). Research has shown that the accuracy of visual inspections is limited (Klerk et al., 2023). Additionally, visual inspections provide information about surface processes, but it is expected that the dominant failure mechanisms are driven by subsurface processes that are not always visible at the surface, such as the two Dutch canal dike failures in 2003. To properly manage risks, water managers should not only focus on visual inspections, but also on monitoring or estimating local subsurface water conditions and associated failure probabilities. This study showed that the *PD* is the best meteorological drought indicator for both soil moisture and groundwater droughts and can be used to organize inspections and substantiate decision-making. Moreover, this indicator can provide valuable insights into subsurface water conditions across various dikes, not only in the Netherlands but also in other countries with similar types of dikes. It can serve as a proxy for subsurface water conditions, allowing for a more substantiated quantification of wetting and drying over the years, when no measurements of the subsurface water conditions are available. This research highlighted the presence of non-hydrostatic pore water pressures in dikes during droughts, which can negatively influence dike safety; the top soil layers dry out, reducing soil weights, while the reduction of deeper pore-water pressures is delayed. This can result in situations where effective stresses are lower than those assumed under hydrostatic conditions. To accurately evaluate dike stability during droughts, safety assessments must take into account these non-hydrostatic conditions.

6. Conclusions and Recommendations

Data analyses were carried out that improved the geohydrological understanding of canal dikes, particularly concerning the development of droughts, and also in wet situations. Observations indicated that hydraulic head levels in canal dikes were very shallow during the winter, with approximately 50% of the monitoring points located on the inner slope and toe of the dike experienced head levels above 20 cm below the surface. These levels are close to the physical maximum, since these are phreatic heads within the dike body and further saturation of soils limits the infiltration of rainfall. During the monitoring period, two extremely dry summers occurred (2020 and 2022) giving valuable insights into the geohydrological extremes, where the minimum and maximum observed groundwater levels can lie almost 2 m apart. These variations occurred while the canal water levels were more or less constant, highlighting the importance of meteorological conditions. The head levels in several dikes were non-hydrostatic during dry summers, which are often not accounted for in dike safety assessments and can worsen the stability during droughts.

Performances of PD and standardized drought indicators (*SPI* and *SPEI*) to estimate subsurface water conditions in dikes were evaluated. The PD appeared to be the most reliable meteorological drought indicator for droughts in canal dikes, for both soil moisture and groundwater droughts. The standardized indicators have limitations for dike safety applications, because they filter out seasonality and express the drought in relative terms, while for dike safety the absolute subsurface water levels are of main interest. Last, the drought recovery was analyzed, which indicates the transition between seasons and the corresponding causes of failure, initiated or affected by varying subsurface water conditions. The soil moisture and groundwater levels following the exceptionally dry summer of 2022 took up to 4.5 months to recover across various locations. This exceeded the onset of the subsequent storm/winter season. Despite heavy precipitation events during the winter season (in January 2023), the previously dried-out soils are able to effectively store the water, thus mitigating potential high hydraulic head levels that are relevant for failure mechanisms in the winter.

Although we showed that meteorological drought indicators can provide information about subsurface water conditions, the use of soil moisture and hydraulic head data directly, or in combination with groundwater models, can help to identify weak spots even more accurately. We encourage taking and sharing multi-year measurements of subsurface water conditions in dikes to create a larger data set to improve our geohydrological understanding and make results and conclusions statistically more significant. Furthermore, to accurately assess the safety of dikes in terms of failure probabilities, the extreme loading conditions (head levels, soil moisture content and suction levels) have to be estimated in terms of probabilities. Multi-year observations are often insufficient to estimate extreme conditions (e.g., the head level with a probability of 1/100 per year), therefore methods to estimate these extreme conditions are necessary. Furthermore, these methods can help to assess how failure probabilities change with changing environmental conditions, like land subsidence and climate change and assess the effectiveness of measures. For example, canal dikes that are prone to droughts are commonly strengthened in practice by covering the dike with a sandy clay layer to (a) increase the weight and height of the dike and (b) to make the underlying peat or organic clay layers less vulnerable to droughts. The impact of this new top layer on the subsurface water conditions is often not incorporated in the design, because lack of reliable measurements and models, despite its potential to affect the effectiveness of measures aimed to reduce failure probabilities.

Data Availability Statement

The following data are available at the 4TU.ResearchData (Strijker, 2023):

- Soil moisture, soil temperature and soil salinity data (Excel-files)
- Hydraulic head data from standpipes (CSV-files)
- Cross-sectional dike profiles (Excel-files)
- Bore profiles (pdf-files in Dutch) and soil characteristics data (Excel-file)
- Rainfall and potential evaporation data (CSV-file)

Readme files are added and describe the data files. The data source has a CC0 license, which entails the waiver of all copyright and related rights, enabling unrestricted use of the data for any purpose. Authors appreciate being informed when using the data by contacting the corresponding author. New data will be added in the future.

References

Aanstoos, J. V., Hasan, K., O'Hara, C. G., Prasad, S., Dabbiru, L., Mahrooghy, M., et. al. (2011). Earthen levee monitoring with synthetic aperture radar. In *2011 IEEE applied imagery pattern recognition workshop (AIPR)* (pp. 1–6).

AghaKouchak, A., Huning, L. S., Sadegh, M., Qin, Y., Markonis, Y., Vahedifard, F., et. al. (2023). Toward impact-based monitoring of drought and its cascading hazards. *Nature Reviews Earth and Environment*, *4*(8), 582–595. https://doi.org/10.1038/s43017-023-00457-2

Beersma, J. J., & Buishand, T. A. (2004). Joint probability of precipitation and discharge deficits in The Netherlands. *Water Resources Research*, *40*(12). https://doi.org/10.1029/2004wr003265

Beersma, J. J., & Buishand, T. A. (2007). Drought in the Netherlands–Regional frequency analysis versus time series simulation. *Journal of Hydrology*, *347*(3–4), 332–346. https://doi.org/10.1016/j.jhydrol.2007.09.042

Berendsen, H. J. A., & Stouthamer, E. (2002). Paleogeographic evolution and avulsion history of the Holocene Rhine-Meuse delta, The Netherlands. *Netherlands Journal of Geosciences*, *81*(1), 97–112. https://doi.org/10.1017/s0016774600020606

Bezuijen, A., Kruse, G. A., & Van, M. A. (2005). Failure of peat dikes in The Netherlands. In *Proceedings of the 16th international conference on soil mechanics and geotechnical engineering* (pp. 1857–1860). IOS Press.

Chlaib, H. K., Mahdi, H., Al-Shukri, H., Su, M. M., Catakli, A., & Abd, N. (2014). Using ground penetrating radar in levee assessment to detect small scale animal burrows. *Journal of Applied Geophysics*, *103*, 121–131. https://doi.org/10.1016/j.jappgeo.2014.01.011

Clark, C. (2002). Measured and estimated evaporation and soil moisture deficit for growers and the water industry. *Meteorological Applications*, *9*(1), 85–93. https://doi.org/10.1017/s1350482702001093

Cundill, S. (2016). Investigation of remote sensing for dike inspection [PhD Thesis]. *University of Twente, Faculty of Geo-Information Science and Earth Observation (ITC)*. https://doi.org/10.3990/1.9789036540360

De Bruin, H. A. R., & Stricker, J. N. M. (2000). Evaporation of grass under non-restricted soil moisture conditions. *Hydrological Sciences Journal*, *45*(3), 391–406. https://doi.org/10.1080/02626660009492337

Dekker, L. W., & Ritsema, C. J. (2000). Wetting patterns and moisture variability in water repellent Dutch soils. *Journal of Hydrology*, *231–232*, 148–164. https://doi.org/10.1016/s0022-1694(00)00191-8

De Lange, W. J., Prinsen, G. F., Hoogewoud, J. C., Veldhuizen, A. A., Verkaik, J., Essink, G. H. O., et al. (2014). An operational, multi-scale, multi-model system for consensus-based, integrated water management and policy analysis: The Netherlands hydrological instrument. *Environmental Modelling and Software*, *59*, 98–108. https://doi.org/10.1016/j.envsoft.2014.05.009

Deyer, M., Utili, S., & Zielinski, M. (2009). Field survey of desiccation fissuring of flood embankments. In *Proceedings of the institution of civil engineers - water management* (Vol. 162(3), 221–232). Thomas Telford Ltd. https://doi.org/10.1680/wama.2009.162.3.221

Elia, G., Cotecchia, F., Pedone, G., Vaunat, J., Vardon, P. J., Pereira, C., et al. (2017). Numerical modelling of slope–vegetation–atmosphere interaction: An overview. *The Quarterly Journal of Engineering Geology and Hydrogeology*, *50*(3), 249–270. https://doi.org/10.1144/qjegh2016-079

Frank, R., Bauduin, C., & Driscoll, R. M. (2004). Designers' guide to Eurocode 7: Geotechnical design: Designers' guide to EN 1997-1. In *Eurocode 7: Geotechnical design-general rules*. Thomas Telford.

Hillel, D. (2003). *Introduction to environmental soil physics*. Elsevier.

Hisdal, H., Stahl, K., Tallaksen, L. M., & Demuth, S. (2001). Have streamflow droughts in Europe become more severe or frequent? *International Journal of Climatology*, *21*(3), 317–333. https://doi.org/10.1002/joc.619

Hooghoudt, S. B. (1940). *Bijdragen tot de kennis van eenige natuurkundige grootheden van den grond: Algemeene beschouwing van het probleem van de detailontwatering en de infiltratie door middel van parallel loopende drains, greppels, slooten en kanalen* (Vol. 46, 14B). Algemeene Landsdrukkerij.

Hubble, T., De Carli, E., & Airey, D. (2014). Geomechanical modeling of the murray's millennium drought river bank failures: A case of the unexpected consequences of slow drawdown, soft bank materials and anthropogenic change. In *Proceedings of the 7th Australian stream management conference* (pp. 278–284). Townsville.

Jamalinia, E., Vardon, P. J., & Steele-Dunne, S. C. (2019). The effect of soil–vegetation–atmosphere interaction on slope stability: A numerical study. *Environmental Geotechnics*, *8*(7), 430–441. https://doi.org/10.1680/jenge.18.00201

Jamalinia, E., Vardon, P. J., & Steele-Dunne, S. C. (2020). The impact of evaporation induced cracks and precipitation on temporal slope stability. *Computers and Geotechnics*, *122*, 103506. https://doi.org/10.1016/j.compgeo.2020.103506

Jevrejeva, S., Jackson, L. P., Grinsted, A., Lincke, D., & Marzeion, B. (2018). Flood damage costs under the sea level rise with warming of 1.5 C and 2 C. *Environmental Research Letters*, *13*(7), 074014. https://doi.org/10.1088/1748-9326/aacc76

Kchouk, S., Melsen, L. A., Walker, D. W., & van Oel, P. R. (2021). A review of drought indices: Predominance of drivers over impacts and the importance of local context. *Natural Hazards and Earth System Sciences Discussions*, *2021*, 1–28.

Klerk, W. J., Kanning, W., Kok, M., Bronsveld, J., & Wolfert, A. R. M. (2023). Accuracy of visual inspection of flood defences. *Structure and Infrastructure Engineering*, *19*(8), 1076–1090. https://doi.org/10.1080/15732479.2021.2001543

Kong, L. W., Bai, W., & Guo, A. G. (2012). Effects of cracks on the electrical conductivity of a fissured laterite: A combined experimental and statistical study. *Geotechnical Testing Journal*, *35*(6), 870–878. https://doi.org/10.1520/gtj20120070

Lendering, K., Schweckendiek, T., & Kok, M. (2018). Quantifying the failure probability of a canal levee. *Georisk: Assessment and Management of Risk for Engineered Systems and Geohazards*, *12*(3), 203–217. https://doi.org/10.1080/17499518.2018.1426865

Lendering, K. T. (2018). *Advancing methods for evaluating flood risk reduction measures*. Doctoral dissertation, Delft University of Technology.

Liu, L., Gudmundsson, L., Hauser, M., Qin, D., Li, S., & Seneviratne, S. I. (2019). Revisiting assessments of ecosystem drought recovery. *Environmental Research Letters*, *14*(11), 114028. https://doi.org/10.1088/1748-9326/ab4c61

Lloyd-Hughes, B. (2014). The impracticality of a universal drought definition. *Theoretical and Applied Climatology*, *117*(3), 607–611. https://doi.org/10.1007/s00704-013-1025-7

Manh, N. V., Merz, B., & Apel, H. (2013). Sedimentation monitoring including uncertainty analysis in complex floodplains: A case study in the Mekong delta. *Hydrology and Earth System Sciences*, *17*(8), 3039–3057. https://doi.org/10.5194/hess-17-3039-2013

Martín-Antón, M., Negro, V., del Campo, J. M., López-Gutiérrez, J. S., & Esteban, M. D. (2016). Review of coastal land reclamation situation in the world. *Journal of Coastal Research*, *75*(10075), 667–671. https://doi.org/10.2112/si75-133.1

McKee, T. B., Doesken, N. J., & Kleist, J. (1993). The relationship of drought frequency and duration to time scales. *Proceedings of the 8th conference on applied climatology* (Vol. 17(22), 179–183).

Meter Group. (2021). TEROS 11/12 manual web. Retrieved from https://publications.metergroup.com/Manuals/20587_TEROS11-12_Manual_Web.pdf

Morton, L. W., & Olson, K. R. (2018). The pulses of the Mekong river basin: Rivers and the livelihoods of farmers and Fishers. *Journal of Environmental Protection*, *9*(04), 431–459. https://doi.org/10.4236/jep.2018.94027

Muñoz-Sabater, J., Dutra, E., Agustí-Panareda, A., Albergel, C., Arduini, G., Balsamo, G., et al. (2021). ERA5-Land: A state-of-the-art global reanalysis dataset for land applications. *Earth System Science Data*, *13*(9), 4349–4383. https://doi.org/10.5194/essd-13-4349-2021

Neuzil, C. E. (1986). Groundwater flow in low-permeability environments. *Water Resources Research*, *22*(8), 1163–1195. https://doi.org/10.1029/wr022i008p01163

O'Dell, J., Nienhuis, J. H., Cox, J. R., Edmonds, D. A., & Scussolini, P. (2021). A global open-source database of flood-protection levees on river deltas (openDELvE). *Natural Hazards and Earth System Sciences Discussions*, 1–16.

Oude Essink, G. H. P., Van Baaren, E. S., & De Louw, P. G. (2010). Effects of climate change on coastal groundwater systems: A modeling study in The Netherlands. *Water Resources Research*, *46*(10). https://doi.org/10.1029/2009wr008719

Özer, I. E., Rikkert, S. J., van Leijen, F. J., Jonkman, S. N., & Hanssen, R. F. (2019). Sub-seasonal levee deformation observed using satellite radar interferometry to enhance flood protection. *Scientific Reports*, *9*(1), 1–10. https://doi.org/10.1038/s41598-019-39474-x

Özer, I. E., van Damme, M., & Jonkman, S. N. (2019). Towards an international levee performance database (ILPD) and its use for macro-scale analysis of levee breaches and failures. *Water*, *12*(1), 119. https://doi.org/10.3390/w12010119

Philip, S. Y., Kew, S. F., Van Der Wiel, K., Wanders, N., & Van Oldenborgh, G. J. (2020). Regional differentiation in climate change induced drought trends in The Netherlands. *Environmental Research Letters*, *15*(9), 094081. https://doi.org/10.1088/1748-9326/ab97ca

Pigott, P. T., Hanrahan, E. T., & Somers, N. (1992). Major canal reconstruction in peat areas. *Water Maritime and Energy*, *96*(3), 141–152. https://doi.org/10.1680/iwtme.1992.21082

Pleijster, E. J., van der Veeken, C., Jongerius, R., & Luiten, E. (2015). Dijken van Nederland. Nai010 uitgevers.

Rentschler, J., Salhab, M., & Jafino, B. A. (2022). Flood exposure and poverty in 188 countries. *Nature Communications*, *13*(1), 1–11. https://doi.org/10.1038/s41467-022-30727-4

Ridley, A., McGinnity, B., & Vaughan, P. (2004). Role of pore water pressures in embankment stability. *Proceedings of the Institution of Civil Engineers-Geotechnical Engineering* (Vol. 157(4), 193–198). https://doi.org/10.1680/geng.2004.157.4.193

Rikkert, S. J. H. (2022). *A system perspective on flood risk in polder drainage canal systems*. Doctoral dissertation, Delft University of Technology.

Robinson, J. D., & Vahedifard, F. (2016). Weakening mechanisms imposed on California's levees under multiyear extreme drought. *Climatic Change*, *137*(1–2), 1–14. https://doi.org/10.1007/s10584-016-1649-6

Schulte, R. P. O., Diamond, J., Finkele, K., Holden, N. M., & Brereton, A. J. (2005). Predicting the soil moisture conditions of Irish grasslands. *Irish Journal of Agricultural & Food Research*, 95–110.

Schwalm, C. R., Anderegg, W. R., Michalak, A. M., Fisher, J. B., Biondi, F., Koch, G., et al. (2017). Global patterns of drought recovery. *Nature*, *548*(7666), 202–205. https://doi.org/10.1038/nature23021

Senatilleke, U., Sirisena, J., Gunathilake, M. B., Muttil, N., & Rathnayake, U. (2023). Monitoring the meteorological and hydrological droughts in the largest river basin (Mahaweli River) in Sri Lanka. *Climate*, *11*(3), 57. https://doi.org/10.3390/cli11030057

Shao, W., Bogaard, T. A., Bakker, M., & Greco, R. (2015). Quantification of the influence of preferential flow on slope stability using a numerical modelling approach. *Hydrology and Earth System Sciences*, *19*(5), 2197–2212. https://doi.org/10.5194/hess-19-2197-2015

Sharp, M., Wallis, M., Deniaud, F., Hersch-Burdick, R., Tourment, R., Matheu, E., et al. (2013). The international levee handbook.

Stirling, R. A., Toll, D. G., Glendinning, S., Helm, P. R., Yildiz, A., Hughes, P. N., & Asquith, J. D. (2021). Weather-driven deterioration processes affecting the performance of embankment slopes. *Géotechnique*, *71*(11), 957–969. https://doi.org/10.1680/jgeot.19.sip.038

Strijker, B. (2023). Multi-year monitoring data of subsurface water conditions for Dutch canal dikes. Version 1. 4TU [Dataset]. *ResearchData*. https://doi.org/10.4121/136aa5df-1907-43ac-a5b0-e0ea8f2dedf3.v1

TAW. (2004). Technisch rapport waterspanningen bij dijken Waterkeringen (TAW).

Tran, D. D., & Weger, J. (2018). Barriers to implementing irrigation and drainage policies in an giang province, mekong delta, Vietnam. *Irrigation and Drainage*, *67*(S1), 81–95. https://doi.org/10.1002/ird.2172

Triet, N. V. K., Dung, N. V., Fujii, H., Kummu, M., Merz, B., & Apel, H. (2017). Has dyke development in the Vietnamese Mekong Delta shifted flood hazard downstream? *Hydrology and Earth System Sciences*, *21*(8), 3991–4010. https://doi.org/10.5194/hess-21-3991-2017

U.S. Army Corps of Engineers. (2003). *Slope stability–engineering manual. Technical report*. Army Corps of Engineers. Retrieved from https://www.publications.usace.army.mil/Portals/76/Publications/EngineerManuals/EM_1110-2-1902.pdf

Vahedifard, F., Robinson, J. D., & AghaKouchak, A. (2016). Can protracted drought undermine the structural integrity of California's earthen levees? *Journal of Geotechnical and Geoenvironmental Engineering*, *142*(6), 02516001. https://doi.org/10.1061/(asce)gt.1943-5606.0001465

Van Baars, S. (2005). The horizontal failure mechanism of the Wilnis peat dyke. *Géotechnique*, *55*(4), 319–323. https://doi.org/10.1680/geot.55.4.319.65491

Van Baars, S., & Van Kempen, I. M. (2009). *The causes and mechanisms of historical dike failures in The Netherlands* (pp. 1–14). E-Water Official Publication of the European Water Association.

van der Meulen, M. J., van der Spek, A. J., de Lange, G., Gruijters, S. H., van Gessel, S. F., Nguyen, B. L., et al. (2007). Regional sediment deficits in the Dutch lowlands: Implications for long-term land-use options (8 pp). *Journal of Soils and Sediments*, *7*(1), 9–16. https://doi.org/10.1065/jss2006.12.199

Van der Wiel, K., Beersma, J., van den Brink, H., Krikken, F., Selten, F., Severijns, C., et al. (2024). KNMI'23 climate scenarios for The Netherlands: Storyline scenarios of regional climate change. *Earth's Future*, *12*(2), e2023EF003983. https://doi.org/10.1029/2023ef003983

Van Esch, J. M. (2012). Modeling groundwater flow through embankments for climate change impact assessment. In *Proceedings, 19th international conference on computational methods in water Resources (CMWR 2012)*. University of Illinois at Urbana.

Van Essen. (2016). Diver product manual. Retrieved from https://www.vanessen.com/wp-content/uploads/2022/04/TD-Diver-DI8xx-ProductManual-en.pdf

Van Loon, A. F. (2015). Hydrological drought explained. *Wiley Interdisciplinary Reviews: Water*, *2*(4), 359–392. https://doi.org/10.1002/wat2.1085

Vardon, P. J. (2015). Climatic influence on geotechnical infrastructure: A review. *Environmental Geotechnics*, *2*(3), 166–174. https://doi.org/10.1680/envgeo.13.00055

Vicente-Serrano, S. M., Beguería, S., & López-Moreno, J. I. (2010). A multiscalar drought index sensitive to global warming: The standardized precipitation evapotranspiration index. *Journal of Climate*, *23*(7), 1696–1718. https://doi.org/10.1175/2009jcli2909.1

Vrijling, J. K. (2001). Probabilistic design of water defense systems in The Netherlands. *Reliability Engineering and System Safety*, *74*(3), 337–344. https://doi.org/10.1016/s0951-8320(01)00082-5

Warner, J. F., van Staveren, M. F., & van Tatenhove, J. (2018). Cutting dikes, cutting ties? Reintroducing flood dynamics in coastal polders in Bangladesh and The Netherlands. *International Journal of Disaster Risk Reduction*, *32*, 106–112. https://doi.org/10.1016/j.ijdrr.2018.03.020

Wolff, R. G., & Olsen, H. W. (1968). Piezometer for monitoring rapidly changing pore pressures in saturated clays. *Water Resources Research*, *4*(4), 839–843. https://doi.org/10.1029/wr004i004p00839

Wolters, E., Hakvoort, H., Bosch, S., Versteeg, R., Bakker, M., Heijkers, J., et al. (2013). Meteobase: Online neerslag-en referentiegewasverdampingsdatabase voor het Nederlandse waterbeheer. *Meteorologica*, *1*, 15–18.

Wright, S. (1921). Correlation and causation. *Journal of Agricultural Research*, *20*, 557–585.

Zhang, J. M., Luo, Y., Zhou, Z., Chong, L., Victor, C., & Zhang, Y. F. (2021). Effects of preferential flow induced by desiccation cracks on slope stability. *Engineering Geology*, *288*, 106164. https://doi.org/10.1016/j.enggeo.2021.106164